AGU PUBLICATIONS

Paleoceanography

RESEARCH ARTICLE
10.1002/2013PA002584

Key Points:
- Shallow waters in southwest Pacific change source location in deglaciation
- Source waters in southwest Pacific switched from high to low latitude since LGM

Supporting Information:
- Supplemental Table S1 and Figures S1–S3

Correspondence to:
E. L. Sikes,
sikes@marine.rutgers.edu

Citation:
Schiraldi, B., Jr., E. L. Sikes, A. C. Elmore, M. S. Cook, and K. A. Rose (2014), Southwest Pacific subtropics responded to last deglacial warming with changes in shallow water sources, *Paleoceanography*, *29*, 595–611, doi:10.1002/2013PA002584.

Received 14 NOV 2013
Accepted 21 MAY 2014
Accepted article online 26 MAY 2014
Published online 17 JUN 2014

Southwest Pacific subtropics responded to last deglacial warming with changes in shallow water sources

Benedetto Schiraldi Jr.[1], Elisabeth L. Sikes[1], Aurora C. Elmore[1,2], Mea S. Cook[3], and Kathryn A. Rose[4]

[1]Institute of Marine and Coastal Science, Rutgers University, New Brunswick, New Jersey, USA, [2]Now at Department of Geography, Durham University, Durham, UK, [3]Geosciences Department, Williams College, Williamstown, Massachusetts, USA, [4]Department of Geology and Geophysics, Woods Hole Oceanographic Institution, Woods Hole, Massachusetts, USA

Abstract This study examined sources of mixed layer and shallow subsurface waters in the subtropical Bay of Plenty, New Zealand, across the last deglaciation (~30–5 ka). $\delta^{18}O$ and $\delta^{13}C$ from planktonic foraminifera *Globgerinoides bulloides* and *Globorotalia inflata* in four sediment cores were used to reconstruct surface mixed layer thickness, $\delta^{18}O$ of seawater ($\delta^{18}O_{SW}$) and differentiate between high- and low-latitude water provenance. During the last glaciation, depleted planktonic $\delta^{18}O_{SW}$ and enriched $\delta^{13}C$ (−0.4–0.1‰) indicate surface waters had Southern Ocean sources. A rapid $\delta^{13}C$ depletion of ~1‰ in *G. bulloides* between 20 and 19 ka indicates an early, permanent shift in source to a more distal tropical component, likely with an equatorial Pacific contribution that persisted into the Holocene. At 18 ka, a smaller but similar shift in *G. inflata* $\delta^{13}C$ depletion of ~0.3‰ suggests that deeper subsurface waters had a delayed reaction to changing conditions during the deglaciation. This contrasts with the isotopic records from nearby Hawke Bay, to the east of the North Island of New Zealand, which exhibited several changes in thermocline depth indicating switches between distal subtropical and proximal subantarctic influences during the early deglaciation ending only after the Antarctic Cold Reversal. Our results identify the midlatitude subtropics, such as the area around the North Island of New Zealand, as a key region to decipher high- versus low-latitude influences in Southern Hemisphere shallow water masses.

1. Introduction

A key to understanding the driving forces in the climate system is determining how these forces manifested themselves regionally in past climate modes. Natural changes in climate can be recorded by environmental archives, which preserve some characteristics of past environmental conditions. By providing us with a glimpse of past atmospheric and oceanic conditions, climate proxy records have been fundamental in providing information about past climate variability.

The Last Glacial Maximum (LGM) ended with warming in the Southern Hemisphere that is accepted to have led the Northern Hemisphere [*Blunier et al.*, 1998; *Shakun et al.*, 2012; *Sowers and Bender*, 1995; *Stott et al.*, 2007]. Despite consensus about the relative timing of Southern versus Northern Hemisphere deglacial events, the forcing mechanisms linking Southern and Northern Hemisphere deglacial events with those in the tropics are still being debated in the paleoclimate community [e.g., *Huybers and Denton*, 2008; *Ninnemann and Charles*, 1997; *Spero and Lea*, 2002]. One way to examine the relationship between high- and low-latitude climate changes is by studying midlatitude climate records across periods of significant climate change [*Bostock et al.*, 2004; *Carter et al.*, 2008; *Pahnke and Sachs*, 2006; *Spero and Lea*, 2002].

The last deglacial transition was marked by major changes in ocean and atmospheric circulation patterns [*Anderson et al.*, 2009; *Bush and Philander*, 1999; *Pahnke and Zahn*, 2005; *Toggweiler*, 1999; *Toggweiler et al.*, 2006]. During the LGM, global deep ocean circulation differed from today with diminished meridional overturning circulation accompanied by decreased upwelling in the Southern Ocean [e.g., *Anderson et al.*, 2009] and reduced ventilation of the abyssal ocean [e.g., *Sikes et al.*, 2000]. A number of mechanisms have been proposed to explain these circulation variations including a weakening and northward shift in the Southern Hemisphere westerlies [*Sigman et al.*, 2010; *Toggweiler*, 1999; *Toggweiler et al.*, 2006].

The surface waters around northern New Zealand today are subtropical with generalized surface flow transiting across the Tasman Sea [*Hamilton*, 2006] coalescing into the southeastward flowing East Auckland

Current (EAUC) along the northern edge of the North Island delivering waters to the Bay of Plenty. The delineation of the shallow interior water masses in this region and all their subcategories is a complex issue, heavily steeped in semantics and with a lot of uncertainty as to provenance and extent, but a generalized picture can be painted. The dominant subsurface water mass transported from the Tasman is Subtropical Mode Water (STMW) carried in the same generalized flow (Figure 1). Flow out of the Bay of Plenty rounds the East Cape of the North Island as the East Cape Current (ECC), which has an attendant coastal counter current and permanent eddies that sit to the east of the North Island [*Chiswell,* 2003, 2005]. The southward flowing ECC deflects east as it hits the Chatham Rise, meeting up with the northward flowing Southland Current, and converging into the Subtropical Front (STF).

The STF marks the northernmost edge of the Southern Ocean [*Belkin and Gordon*, 1996; *Orsi et al.*, 1995]. East of New Zealand, the latitudinal location of the STF is bathymetrically fixed by the Chatham Rise at ~42°S [*Belkin and Gordon*, 1996; *Chiswell*, 1994; *Heath*, 1985]. South of the STF, Subantarctic Surface Water (SAW) sits at the surface. Farther south in the Southern Ocean, the Subantarctic Front (SAF) marks the northern edge of the Antarctic Circumpolar Current (ACC) and the northern edge of the formation region of Antarctic Intermediate water (AAIW). Here colder fresher polar waters advect north below SAMW [*McCartney*, 1977; *Sloyan and Rintoul*, 2001; *Tsuchiya and Talley*, 1996]. North of this front, Subantarctic Mode Water (SAMW) is formed by deep winter mixing [*McCartney*, 1977; *Sloyan and Rintoul*, 2001; *Tsuchiya and Talley*, 1996]. Both AAIW and SAMW sink below less dense surface layers as they advect to the north (Figure 1b). North of the STF, AAIW sits between 500 and 1500 m water depth, characterized by a salinity minimum (Figure 1b) and SAMW as a thermostad at roughly 200–500 m water depth [*McCartney*, 1977]. Both are characterized by enriched $\delta^{13}C$ relative to deep water masses (Figure 1c). Recent analysis confirms the broad formation of SAMW and AAIW across the breadth of the Pacific region of the Southern Ocean, with different formation regions and processes producing SAMW and AAIW with distinct properties arising from different locations [*Bostock et al.*, 2013; *Sokolov and Rintoul*, 2000]. AAIW filling the Tasman Sea, to the west of New Zealand, is saltier than AAIW formed in the east Pacific (as reviewed in *Bostock et al.* [2013]) and SAMW is warmer [*Sokolov and Rintoul*, 2000]. This suggests two possible source paths for AAIW and the possible influence of SAMW overlying it into the Bay of Plenty [*Sokolov and Rintoul*, 2000].

In the Southern Ocean, strong westerly winds drive the ACC, causing deep isopycnal mixing [*Orsi et al.*, 1995; *Rintoul and Bullister*, 1999; *Sallée et al.*, 2010] ventilating circumpolar deep water (CDW) and shallower, northward flowing interior water masses. Although the modern surface circulation around northern and eastern New Zealand in our study region is reasonably well characterized [*Belkin and Gordon*, 1996; *Hopkins et al.*, 2010; *Ridgway and Dunn*, 2007; *Ridgway and Hill*, 2009; *Roemmich and Sutton*, 1998], shallow subsurface flows may have multiple paths [*Bostock et al.*, 2010, 2013] that are poorly constrained and may depend on varying conditions in the formation regions. On glacial timescales, changes in frontal locations and deep water sources are known to have affected the formation, characteristics, and sources of subsurface water masses in the study region and throughout the Southern Ocean [e.g., *Charles et al.*, 2010; *Pahnke and Zahn*, 2005]. In the New Zealand region, for example, northward migration and intensification of the SAF under stronger winds resulted in an overall intensification of paleocirculation around the flanks of the Campbell Plateau and increased thermal gradients at the STF that may have fed cool water flows along the eastern North Island [*Carter et al.*, 2008; *Marr et al.*, 2013; *Neil et al.*, 2004; *Sikes et al.*, 2002].

The $\delta^{13}C$ of planktonic foraminifera is a useful tracer for reconstructing subsurface water mass circulation patterns. The dissolved inorganic carbon (DIC) of subsurface water masses becomes depleted, or lower, in $\delta^{13}C$ as they accumulate respired DIC released during remineralization of $\delta^{13}C$-depleted organic carbon. The $\delta^{13}C$-respired CO_2 signal can thus be related to the distance from the site of water mass formation [e.g., *Bostock et al.*, 2010; *Loubere and Bennett*, 2008; *Spero et al.*, 2003]. In the South Pacific Ocean, deeper water masses are relatively depleted in $\delta^{13}C$ owing to the respired CO_2 signal that has accumulated along the long flow path from the North Atlantic [e.g., *Curry and Oppo*, 2005; *Curry et al.*, 1988]. However, shallower water masses reflect substantial reequilibration with the atmosphere while at the surface in the Southern Ocean. The dependence of $\delta^{13}C$ fractionation on temperature during air-sea equilibrium partitioning causes colder waters to have both higher CO_2 content and increased $\delta^{13}C$ [*Mook et al.*, 1974]. The short travel distance from formation keeps the buildup of respired DIC from being significant in the shallow subsurface around New Zealand today (Figure 1b). The use of carbon and oxygen isotope values of different species of foraminifera

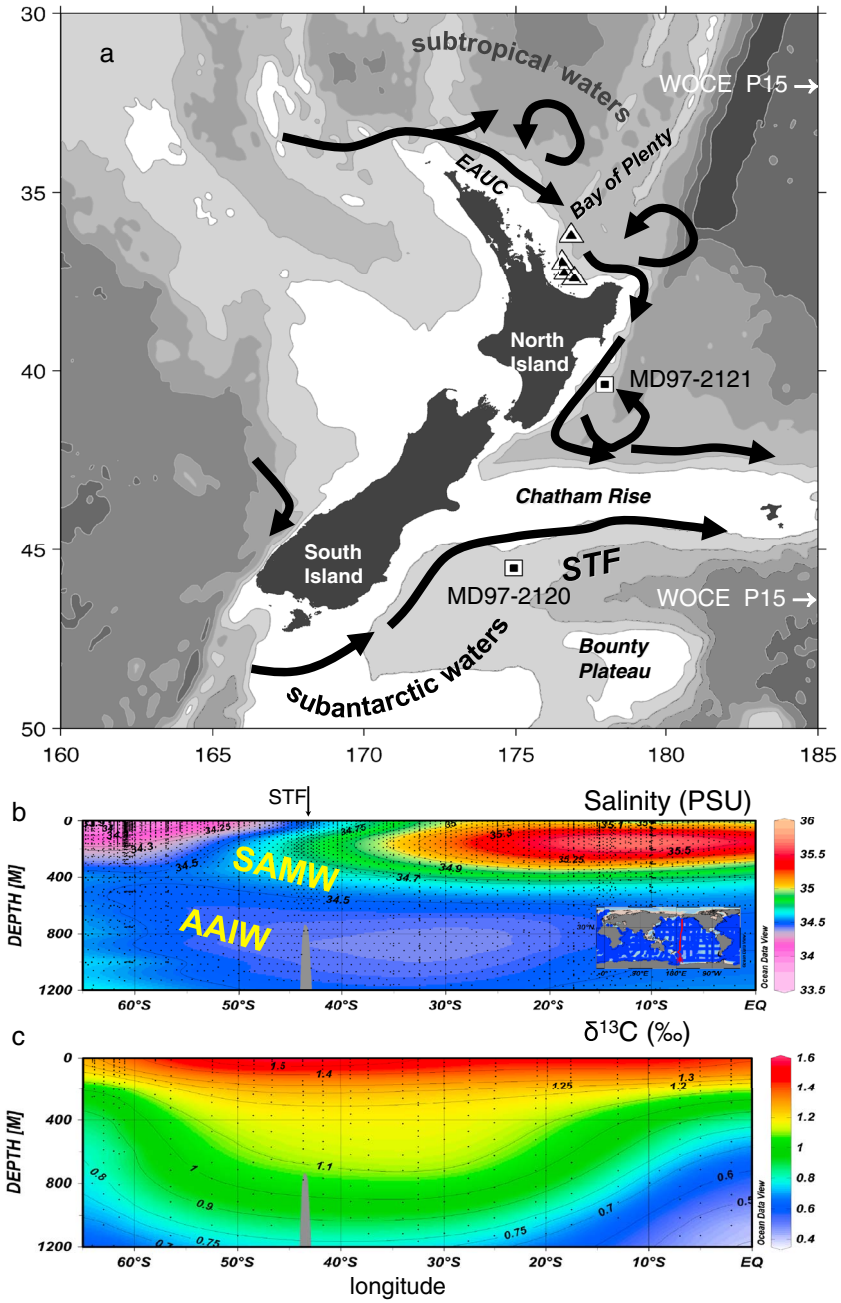

Figure 1. Schematic map and vertical cross sections of modern shallow surface circulation surrounding New Zealand. (a) Surface currents indicated by black arrows. Flow from the Tasman Sea advects subtropical water in from the northwest and coalesces into the East Auckland Current (EAUC) delivering shallow waters to the Bay of Plenty. Continued flow around East Cape delivers subtropical water to Hawke Bay. Subtropical waters are bounded to the south by subantarctic waters of the Southern Ocean separated by the Subtropical Front (STF). Semipermanent eddies off East Cape and north of the Chatham Rise serve to actively recirculate water. New data presented in this study are from cores in the Bay of Plenty (triangles; Table 1). Previously published records from Hawke Bay core MD97-2121 [*Carter et al.*, 2008] and south Chatham Rise core MD97-2120 (squares) [*Pahnke et al.*, 2003] that are discussed in the text are presented for context. (b) Vertical cross section of salinity above 1200 m from WOCE section P15 which sits just to the east of region in the map (indicated by arrows in Figure 1a). Note that surface and shallow waters at latitude of the study area (~35°S) sit in the region with a strong gradient at shallow depths. (c) Vertical cross section of $\delta^{13}C$ above 1200 m section P15. There is no indication of along-transport accumulation of respired CO_2 in these shallow layers. $\delta^{13}C$ values are primarily associated with signatures obtained at formation.

from a single core can be used to cancel out global and regional effects, with the aim of highlighting vertical differences in water properties [e.g., *Curry and Crowley*, 1987]. Comparing records from different sites within the same timeframe allows changes in water mass distribution between sites [e.g., *Neil et al.*, 2004] and the relative contributions from different sources to be distinguished [e.g., *Bostock et al.*, 2004].

In the glaciation, altered circulation caused greater buildup of respired DIC in deep waters, depleting the ^{13}C of deep waters [*Curry and Oppo*, 2005; *Curry et al.*, 1988]. In the deglaciation, transport of depleted terrestrial carbon caused a slow ~0.3‰ decrease in the whole ocean $\delta^{13}C$. This was also accompanied by a more rapid $\delta^{13}C$ depletion cycle in the shallow interior and subsurface water masses of the subtropical Pacific and subantarctic regions of the Southern Ocean that resulted in an isotopic minimum event centered at ~15 ka [*Anderson et al.*, 2009; *Bostock et al.*, 2004; *Carter et al.*, 2008; *Pahnke and Zahn*, 2005; *Pahnke and Sachs*, 2006; *Spero and Lea*, 2002] that closely followed the initiation of the Southern Ocean upwelling system [*Anderson et al.*, 2009]. It has been suggested that these isotopic depletions may have been a direct result of the upwelling of a low $\delta^{13}C$ signal from deeper depths being transmitted throughout the Pacific Ocean via SAMW and AAIW [*Spero and Lea*, 2002], which also caused a deglacial isotopic depletion in atmospheric CO_2 [*Schmitt et al.*, 2012].

The degree to which the isotopic composition of foraminifera tracks the isotopic composition of the local water mass has been established for the southwest Pacific Ocean [*King and Howard*, 2004]. *Globigerina bulloides* and *Globigerina inflata* are widespread nonsymbiont-bearing planktonic foraminiferal species in the southwestern Pacific Ocean used in this study [*Bé*, 1977]. *G. bulloides* is a spinose species of foraminifera, which has been shown to live in the shallow base of the mixed layer in subpolar transitional zones [*Bé*, 1977; *Bé and Tolderlund*, 1971; *Darling et al.*, 2006; *Hemleben et al.*, 1985]. Conversely, *G. inflata* is a nonspinose foraminifera that prefers to live at the base of the thermocline influenced by subsurface waters and dominates subantarctic and subtropical transitional zones [*Bé*, 1977; *Cléroux et al.*, 2007]. The amplitude of the isotopic signal in *G. bulloides* over the annual cycle is similar to the $\delta^{18}O$ range of the modern surface ocean, suggesting that these foraminifera live in the shallowest 50–100 m of the water column, and the isotopic amplitude of *G. inflata* suggests that this species live at greater than 100 m depth down to 300 m [*Field*, 2004; *King and Howard*, 2005]. Comparison with the predicted $\delta^{18}O$ values of the surface waters in the New Zealand sector suggests that *G. inflata* records the actual $\delta^{18}O$ value of the water that it inhabits, whereas *G. bulloides* has a constant $\delta^{18}O$ offset from seawater of roughly 0.4‰ [*King and Howard*, 2005]. Both species have a constant disequilibrium offsets from the $\delta^{13}C$ of DIC of 1.5‰ and 0.3‰ for *G. bulloides* and *G. inflata*, respectively [*King and Howard,* 2001, 2004, 2005].

In this study, high-resolution stable isotopic records from four cores in the Bay of Plenty were compiled to examine changes in shallow interior water masses from the LGM into the Holocene. Two isotopes, $\delta^{13}C$ and $\delta^{18}O$, of two planktonic foraminiferal species that grow at different depths, *G. bulloides* and *G. inflata*, were compared to examine deglacial water mass provenance changes and surface stratification in the subtropical New Zealand region. These records are then compared to nearby Hawke Bay and the south Chatham Rise to create a regional deglacial reconstruction of surface and shallowest subsurface water masses. This study focuses on the midlatitudes, such as New Zealand, as a region that is at a crossroads between high- and low-latitude influence in the Southern Hemisphere.

2. Methods

2.1. Geochemical Methods

An ensemble of four sediment cores (Table 1) from the Bay of Plenty, off the eastern coast of northern New Zealand, was chosen for this study (Figure 1). The sampling intervals varied between 1, 4, and 8 cm, depending on sedimentation rates in the individual cores, and sampling resolution was increased across intervals of interest to this study. Sediment was oven-dried at 30°C overnight, weighed, and wet sieved to 63 μm and the weight of the coarse fraction (>63 μm) was recorded. The planktonic foraminiferal species *G. bulloides* and *G. inflata* were handpicked from 250 to 350 μm size fraction. Stable carbon and oxygen isotopes were analyzed on a Micromass Optima Isotope Ratio mass spectrometer with a multiprep device for automated analyses at Rutgers University Department of Earth Sciences Stable Isotope Laboratory. The mass spectrometer has an analytical precision of 0.08‰ for $\delta^{18}O$ and 0.04‰ for $\delta^{13}C$ ($\pm 1\sigma$), based on the repeated

Table 1. Core Locations

Core Number	Latitude	Longitude	Water Depth (m)	Core Length (cm)
RR0503 64 JPC	37°25.34′S	177°00.14′E	651	1094
RR0503 79 JPC	36°57.52′S	176°35.57′E	1165	663.5
RR0503 87 JPC	37°15.81′S	176°39.86′E	663	894
RR0503 125 JPC	36°11.90′S	176°53.35′E	2541	939

analysis of an in-house standard. Numerical data from this research will be archived in the NOAA National Climatic Data Center (NCDC) database (http://www.ncdc.noaa.gov/data-access/paleoclimatology-data).

The $\delta^{18}O$ signal of subsurface ocean water ($\delta^{18}O_{SW}$) is a conservative tracer that has embedded within it a latitudinal and a salinity component caused by Rayleigh distillation of surface waters, which can be used to estimate source location of subsurface waters. Sea surface temperature (SST) was estimated in using the Mg/Ca ratio of *G. bulloides* from the Bay of Plenty (see the supporting information). The thermal effect on $\delta^{18}O$ of calcite was estimated using the equation of *Shackleton* [1974] and the effect of ice volume was removed using the sea level reconstruction of [*Peltier and Fairbanks*, 2006]. Errors were propagated from uncertainties in the variables input into $\delta^{18}O$ sea level estimation, the $\delta^{18}O$ of *G. bulloides*, and the Mg/Ca calibration. One-sigma error bar of ±0.2‰ associated with errors in the estimations translated through the $\delta^{18}O_{SW}$ calculation were determined. Full calculations are reported in the supporting information. The $\delta^{18}O$ offset between *G. bulloides* and from seawater of roughly 0.4‰ [*King and Howard*, 2005] was not corrected for in our thermocline determinations.

Bioturbation may differentially sort populations of foraminifera when they have differing abundances [*Guinasso and Shink,* 1975; *Peng and Broecker*, 1984]. The possible effect of changes in abundance and/or differential bioturbation causing offsets in the timing of events between the isotopes of the two planktonic species was assessed using assemblage counts of *G. bulloides*, *G. inflata*, *Neogloboquadrina pachyderma* (left coiling), and *N. pachyderma* (right coiling), according to the established taxonomy [*Bé and Gilmer*, 1977; *Thompson and Shackleton*, 1980] and counting methodologies [*Samson et al.*, 2005; *Sikes and Keigwin,* 1994, 1996]. A bioturbation model was used to verify empirically whether bioturbation affected the relative timing of the deglacial onset in the *G. bulloides* and *G. inflata*. An ideal model of isotopic values was developed in which the deglacial shift in isotopic values of *G. bulloides* and *G. inflata* was kept the same but the population counts were matched to test if a bioturbation impulse function is enough to create an offset in the resulting timing mimicking the observed deglacial onset. The bioturbation model follows the form in published work [*Hutson*, 1980] and was used to verify empirically bioturbation effects on the relative timing of the deglacial onset in *G. bulloides* and *G. inflata*. To account for the varying sampling interval between cores in our Bay of Plenty data set, the population assemblage data were linearly interpolated to represent every 1 cm across the core interval with the idealized isotopic value constructed to have the onset of the glacial termination occur at the same depth and with the bioturbation impulse function created as a Gaussian curve for simplicity (see the supporting information). This simulation confirmed that bioturbation on the changing abundances could not have caused observed offsets in the planktonic deglacial isotopic changes in the cores in this study.

2.2. Stratigraphy

The age models for the four RR0503 cores in this study were based primarily on tephra chronology refined with planktonic $\delta^{18}O$ stratigraphy [e.g., *Rose et al.*, 2010]. The stratigraphy for 64 JPC has been previously published [*Rose et al.*, 2010] with stratigraphy established by methods similar to the present study. For the remainder of the cores, tephra tie points include the Rotomoa tephra (9.42 ka), Waiohau (14.0 ka), Rerewhakaaitu (17.49 ka), and Kawakawa tephra (25.35 ka) based on terrestrial radiocarbon dates [*Lowe et al.*, 2013; *Vandergoes et al.*, 2013] (Table 2). The presence of the major ashes suggests continuous sedimentation through the timeframe of interest (30–10 ka), with the exception of 64 JPC that has a hiatus from ~14.7 to 9.8 ka. Sedimentation rates in the cores ranges between 4.8 and 31 cm/kyr throughout the deglacial and Holocene. A linear sedimentation rate was assumed between all chronological tie points (Figure 2).

To quantitatively compare records from the four geographically nearby cores and achieve a "single site" ensemble for the Bay of Plenty, a matching chronology for each core was created by simple linearly

Table 2. Tephrostratigraphic Tie Points Used in the Development of Age Models[a]

Tephra Age (ka)	64 JPC	79 JPC	87 JPC	125 JPC
Tuhua 6.95		32 cm		
Rotoma 9.42	87 cm	46 cm		
Waiohau 13.75	89 cm	81 cm		
Rerewhakaaitu 17.85	153 cm	187 cm	74 cm	164 cm
Okareka 21.86	307 cm	199 cm		282 cm
Te Rere 25.17	372 cm	289 cm		
Kawkawa 25.358		330 cm	157 cm	346 cm

[a]Ages for the tephras are from *Lowe et al.* [2013]. In core 64 JPC, the Rotoma tephra directly overlies the Waiohau indicating a hiatus of ~4 ka [*Rose et al.*, 2010].

interpolating the varying sampling intervals to a centennial incremented age model from 0 to 30 ka. The isotopic values in cores 87 JPC, 64 JPC, 79 JPC, and 125 JPC were then averaged using the *nanmean* function in MatLab to achieve a composite value or ensemble average for the Bay of Plenty (see the supporting information). This approach allowed us to determine robust trends in our Bay of Plenty isotopic records, particularly given that the *G. bulloides* data were characteristically noisy and the *G. inflata* $\delta^{13}C$ data had very small amplitude changes across the timeframe of interest in the data. The individual records for each core are plotted with the ensemble values in Figure 3. The $\delta^{18}O$ and $\delta^{13}C$ values for each species were interpolated to the same stratigraphy (0–30 ka; $n = 301$) and averaged to create a collective ensemble representative of the Bay of Plenty (Figure 3). Full discussion of individual core records is provided in Schiraldi (unpublished Masters thesis, 2013).

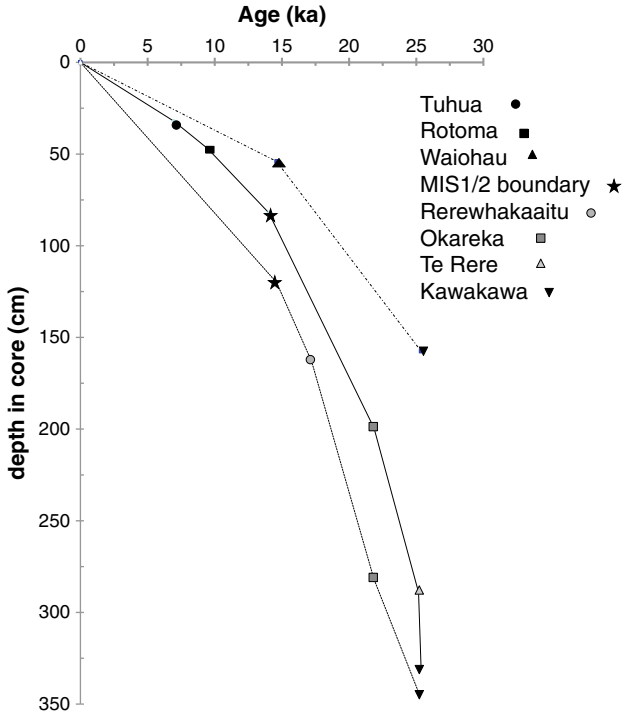

Figure 2. Age depth plots for the cores used in this study. Bay of Plenty cores RR05-03 79 JPC (solid line), 87 JPC (dashed line), and 125 JPC (dotted line). Symbols illustrate stratigraphic tie points for cores from positively identified tephra [*Shane et al.*, 2006] and tephra ages from *Lowe et al.* [2013]. These were combined with marine oxygen isotope stage 1/2 determinations (MIS1/2) at 14.6 ka [*Lisiecki and Raymo*, 2005] in cores 125 JPC and 79 JPC. These combine to create a high-resolution age model for each core.

3. Results

In the three cores that have isotope records extending into the glaciation (87 JPC, 79 JPC, and 125 JPC), the *G. bulloides* ensemble $\delta^{18}O$ record ($\delta^{18}O_{G.\ bulloides}$) increases from 30 to 20 ka by ~0.6‰, with the most enriched values of 2.2 to 2.6‰ occurring just before the termination (20 ka). For core 64 JPC (661 m water depth) [*Rose et al.*, 2010], analyses do not extend into the LGM. The four-core ensemble shows that the deglacial decrease in surface $\delta^{18}O_{G.\ bulloides}$ began at ~20 ka with a steady rise into the Holocene, with a minor plateau at 18 ka. The $\delta^{18}O$ ensemble of the subsurface species, *G. inflata* ($\delta^{18}O_{G.\ inflata}$) shows a similar but smaller late glacial enrichment of about 0.2‰ ending at ~20 ka. The maximum enrichment in all three cores occurred at 17.8 ka, approximately 2 kyr after that seen in the *G. bulloides* record. Thus, the onset of deglacial depletion did not begin in this record until ~17 ka. The glacial to Holocene depletion of 1.2‰ is comparable to the *bulloides* and the Holocene minimum is ~0.7‰ (Figure 3b). The 2 kyr offset in the isotopic onset in the initiation of the

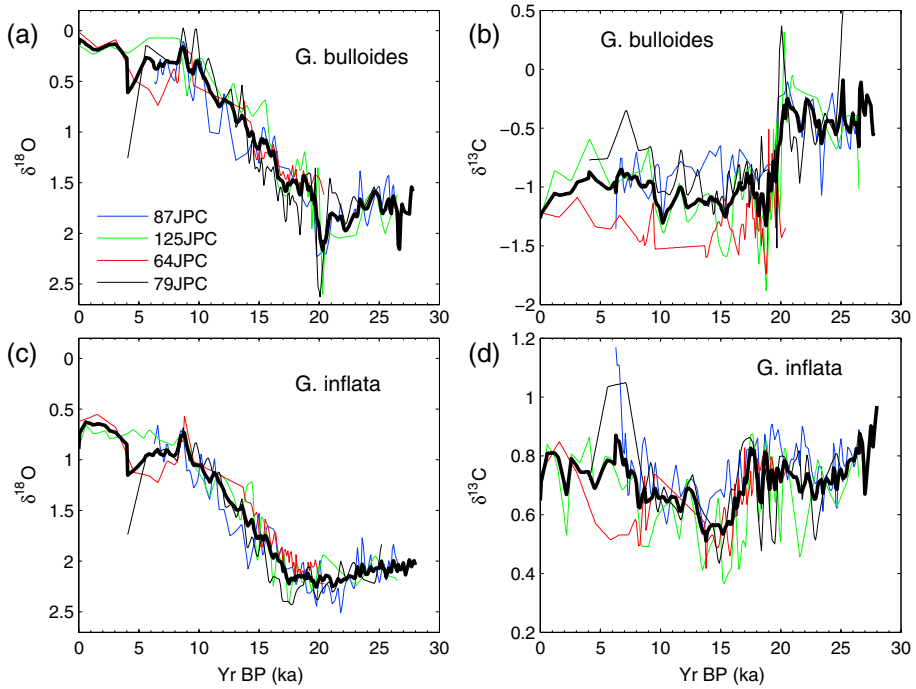

Figure 3. Bay of Plenty $\delta^{18}O$ and $\delta^{13}C$ of planktonic foraminifera in this study. Cores 79 JPC (thin black line), 125 JPC (green), 64 JPC (red), and 87 JPC (blue). (a) $\delta^{18}O$ of *G. bulloides*, (b) $\delta^{13}C$ of *G. bulloides*, (c) $\delta^{18}O$ of *G. inflata*, and (d) $\delta^{13}C$ of *G. inflata*. Stable isotopic data were averaged to produce an ensemble record for each isotope and foraminifera (thick black line).

deglaciation between the *G. bulloides* and *G. inflata* $\delta^{18}O$ records was evaluated for assemblage shifts. It was determined not to be the result of differential bioturbation impacting the foraminiferal isotopic signature and can be considered to be owing to differential oceanographic conditions between the depth habitats of the two species (see the supporting information.)

The $\delta^{13}C$ ensemble average for *G. bulloides* ($\delta^{13}C_{G.\ bulloides}$) in the glaciation was about −0.4‰ with a slight maximum at 20 ka of ~ −0.2‰ at 20 ka (Figure 3c). From 20.1 to 19.1 ka, there was an abrupt depletion event of approximately 1.0‰ in all cores with the minimum ranging from −1.2 to −1.7‰. Core 64 JPC exhibits the same shift, but the onset is not resolvable due to the lack of a complete LGM data set. After the shift, the individual records have a broader range than during the glaciation: cores 79 JPC and 87 JPC averaged ~ −0.9‰ through to the Holocene, while core 125 JPC averaged −1.0‰, and 64 JPC averaged −1.4‰. Despite variability between the four cores, the ensemble average allows for the interpretation of a clear regional trend. The *G. inflata* carbon isotopes and the ensemble ($\delta^{13}C_{G.\ inflata}$) are both more consistent and have less overall noise among cores. The late glacial $\delta^{13}C$ was very steady with only a minor depletion of less than 0.3‰, beginning later, at 17.5 kyr B.P. Unlike $\delta^{13}C_{G.\ bulloides}$, $\delta^{13}C_{G.\ inflata}$ did not exhibit a substantial deglacial shift and showed much smaller changes throughout the record (Figure 3d). In the interval from 25 to 18 kyr B.P., there were no significant trends and the $\delta^{13}C_{G.\ inflata}$ mean was ~0.7‰. During the early deglaciation, from 20 to 16 ka, the ensemble $\delta^{13}C_{G.\ inflata}$ exhibited a gradual depletion of 0.3‰; values plateaued at 0.5‰ until the Antarctic Cold Reversal (ACR), at which point there was an abrupt 0.2‰ enrichment into the Holocene. Values were variable and distinct between cores with mean values of 0.7 - 0.8‰.

The oxygen isotopic composition of planktonic foraminiferal calcite provides information about the oxygen isotope composition of the surface water mass. $\delta^{18}O_{SW}$ can be used in concert with $\delta^{13}C$ to examine changes in the regional subsurface and infer the provenance of the water mass. The largest influences on $\delta^{18}O$ of ocean water ($\delta^{18}O_{SW}$) are the temperature at which the calcite precipitates and the effect of ice volume on the global ocean. Depleted $\delta^{18}O_{SW}$ suggest surface waters were either fresher and/or sourced at higher latitudes during the LGM, than in modern times. Our $\delta^{18}O_{SW}$ reconstructions show significant differences between the LGM and the Holocene with glacial values averaging around −0.2‰ (Figure 4a). At 23 ka there

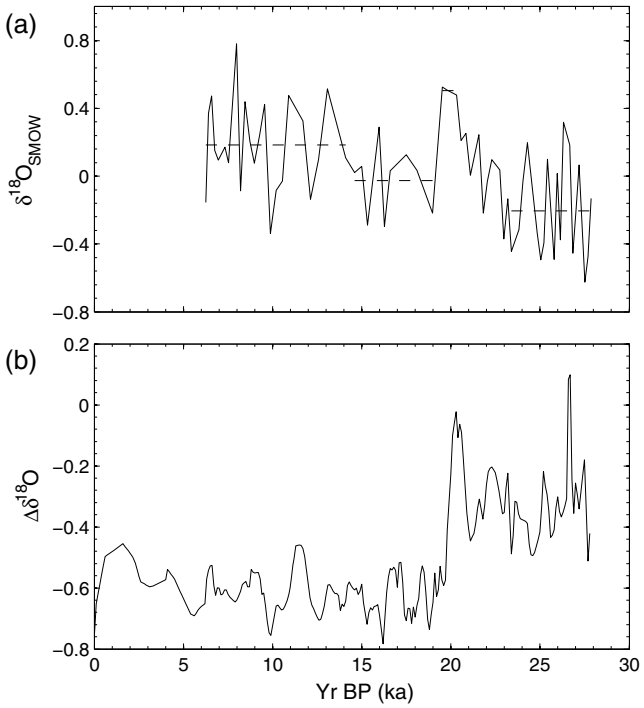

Figure 4. δ^{18}O-derived reconstructions of surface water mass properties. (a) Reconstructed δ^{18}O of seawater (δ^{18}OSW) for core 87 JPC from the Bay of Plenty. Glacial-interglacial ice volume and temperature (estimated using planktonic foraminiferal Mg/Ca) influence on δ^{18}O were removed using published sea level reconstructions [*Peltier and Fairbanks*, 2006] and calculating the temperature effect in calcite [*Shackleton*, 1974]. Three large-scale features in the reconstruction are highlighted (black dashed lines; see text). These features are indicative of surface water mass source variations. (b) $\Delta\delta^{18}$O is the difference between *G. inflata* δ^{18}O and *G. bulloides* δ^{18}O used to estimate the relative depth of the surface mixed layer. Near-zero $\Delta\delta^{18}$O represents similar values in both planktonic species and thus a deeper thermocline; more negative $\Delta\delta^{18}$O suggests a shoaled thermocline.

was an 0.2‰ enrichment with 3 data point maximum of 0.5‰, which persisted until 20 ka. After this event there was a step-change depletion to 0.0‰, which is 0.2‰ more depleted than the LGM. $\delta^{18}O_{SW}$ values remained at this plateau until the ACR. After the ACR, $\delta^{18}O_{SW}$ was highly variable through the Holocene, but on average, values were 0.2‰ more enriched than the LGM. The slow enrichment in the late glaciation and terminal spike at ~20 ka suggest a gradual shift to increasingly low-latitude/saline water advected into the Bay of Plenty late in the glaciation. This was followed by a rapid shift back to high-latitude/fresh water at the onset of the Southern Hemisphere deglaciation. After the shift, the intermediate $\delta^{18}O_{SW}$ values until the ACR suggest a lower latitude mix before increasingly more saline or lower latitude sourced waters gradually became more prevalent in the Bay of Plenty into the Holocene.

The ensemble deglacial response for both δ^{18}O and δ^{13}C of the shallower species, *G. bulloides*, leads that of the deeper subsurface species, *G. inflata*. Bioturbation modeling analysis conducted in two of the cores verifies that this temporal offset is not a result of bioturbation. Therefore, the 2 kyr lag in the timing of the δ^{18}O deglacial onset and the δ^{13}C shift between the species suggests that shallower interior and potentially mixed layer waters experienced a source/compositional change 2 kyr earlier than deeper subsurface waters (Figure 5). The greater magnitude of the δ^{13}C shift in *G. bulloides* suggests a more fundamental change in the mixed layer/shallowest interior water mass that did not occur in the deeper subsurface (Figure 5). Additionally, although shifts in δ^{13}C in planktonic foraminifera in the New Zealand region have been attributed to changes in productivity [*Carter et al.*, 2008], the differences in the deglacial isotopic responses between these two species indicate that the two subsurface depths in the southwest Pacific Ocean were responding to climate and regional forcings, independent of one another. These records indicate that these δ^{13}C changes cannot be attributed to variations in local productivity.

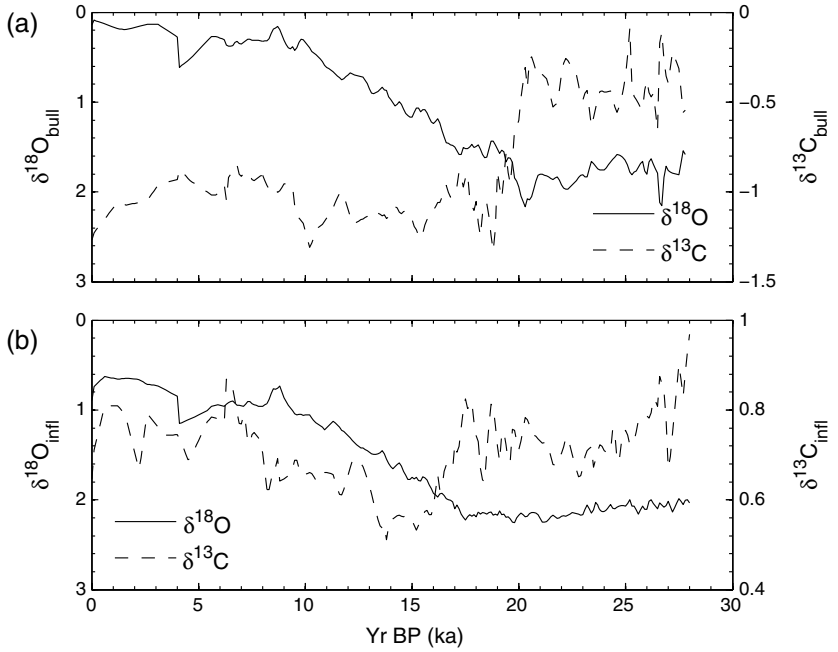

Figure 5. Bay of Plenty ensemble isotopic averages for $\delta^{18}O$ and $\delta^{13}C$. (a) *G. bulloides* $\delta^{18}O$ (solid) and $\delta^{13}C$ (dotted), and (b) *G. inflata* $\delta^{18}O$ (solid) and $\delta^{13}C$ (dotted line). Note that the $\delta^{13}C$ step change in the shallow surface (*G. bulloides* record) begins at ~20 ka, while the subsurface depletion (*G. inflata* record) does not occur until ~17.5 ka. The timing of the deglacial $\delta^{18}O$ shift also occurs at 20 ka in the shallow surface while the subsurface proxy does not change until ~17.5 ka. These temporal differences cannot be a result of preferential bioturbation (see the supporting information).

4. Discussion

4.1. Surface and Subsurface Water Mass Changes in the Bay of Plenty

The initial deglacial $\delta^{18}O$ shift observed in *G. bulloides*, representing the mixed layer to thermocline waters of the Bay of Plenty, occurred before the major change in sea level at 18.5 ka [*Peltier and Fairbanks*, 2006]. Factors known to affect the $\delta^{18}O$ isotopic composition of planktonic foraminifera on glacial to interglacial timescales are the storage of isotopically depleted water in the form of large ice sheets, temperature impacting the thermal incorporation of water $\delta^{18}O$ into the foraminifera test, salinity, and fractionation associated with the source latitude of the interior water mass. With the ice volume signal and glacial-interglacial SST changes in the measured foraminiferal $\delta^{18}O$ removed, the $\delta^{18}O_{SW}$ reconstruction allows a clearer examination of the mixed layer water mass composition. The early $\delta^{18}O_{G.\ bulloides}$ shift coincides with an enrichment pulse in the reconstructed $\delta^{18}O_{SW}$ indicating an increase in temperature and/or salinity in the mixed layer to thermocline waters in the Bay of Plenty at ~20 ka, suggesting a short-term switch from higher-latitude/fresh source waters to a more tropical/saline source at the early onset of deglaciation (Figure 6a).

The difference in the $\delta^{18}O$ values between planktonic foraminiferal species has been used to estimate thermocline depths [e.g., *LaRiviere et al.*, 2012; *Neil et al.*, 2004; *Thornalley et al.*, 2009]. In this study, the difference between *G. inflata* and *G. bulloides* ($\Delta\delta^{18}O$ subsurface-surface) was used to estimate near-surface stratification. Observed differences in offsets between the $\delta^{18}O$ of *G. inflata*, *G. bulloides*, and $\delta^{18}O_{SW}$ in sediment trap studies from the region [*King and Howard*, 2005] suggest that positive values indicate a thicker mixed layer and deep thermocline depths. Subsequently, here $\Delta\delta^{18}O$ values trending negative are interpreted as a shallower thermocline and thinner mixed layer. In the Bay of Plenty, during the late glaciation, $\Delta\delta^{18}O$ values were slightly negative, with a short pulse of values close to zero around 20 ka, indicating that a thick mixed layer (deeper thermocline) was present in the LGM (Figure 4b). At 20.1 ka, at the deglacial onset, a short pulse in $\Delta\delta^{18}O$ toward zero indicates a short interval with an even thicker thermocline, followed by an abrupt shift to values around ~ −0.5‰ indicating a thin mixed layer and shallower thermocline that persisted into the Holocene. Two thermocline modes are clearly evident in this

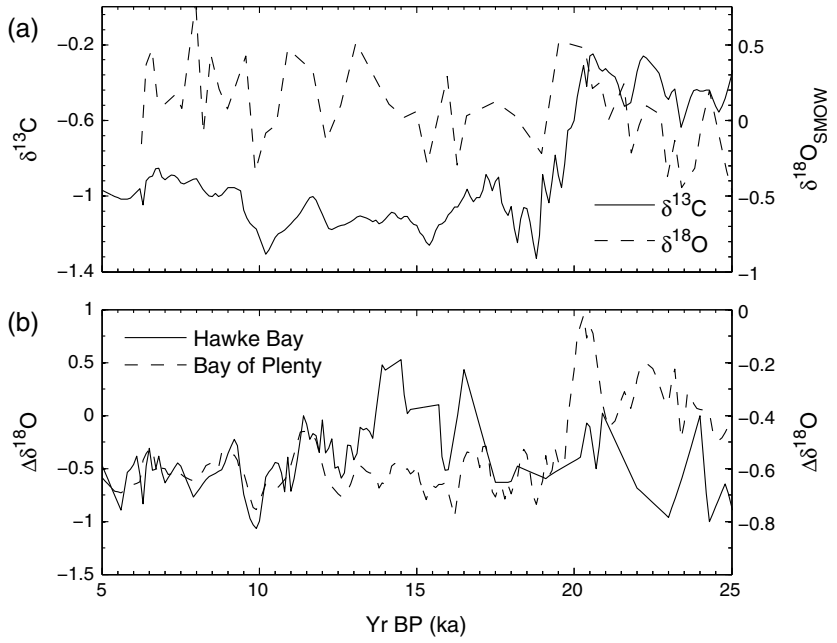

Figure 6. (a) Comparison of deglacial changes in Bay of Plenty surface water proxies with thermocline changes in Hawke Bay for $\delta^{18}O_{SW}$ (dotted line) and *G. bulloides* (surface foraminiferal) $\delta^{13}C$ (solid line) from the Bay of Plenty sediment core 87 JPC. (b) Hawke Bay (solid) and Bay of Plenty (dotted) $\Delta\delta^{18}O$. In the LGM, depleted $\delta^{18}O_{SW}$ and enriched $\delta^{13}C$ in the Bay of Plenty are indicative of high-latitude, fresher, proximal Southern Ocean-dominated source location. In the Holocene, enriched $\delta^{18}O_{SW}$, indicative of a lower latitude and/or more saline waters, is accompanied by depleted $\delta^{13}C$, suggesting a longer flow path and a dominance of waters from more distant/tropical locations.

data set, and a deeper glacial mode dominant prior to 20.1 ka suggests a thicker surface package overlaying subsurface waters with possibly similar salinities (perhaps analogous to conditions today at ~42°; see Figure 1b). A swift and enduring shift to a shallower postglacial mode at 19.5 ka was possibly driven by the pulse of tropical water indicated by the $\delta^{18}O_{SW}$ (discussed above) that reset the system and persisted through to the Holocene where a thin surface layer overlies a stronger pycnocline today (conditions analogous to ~34°S in Figure 1b today).

The planktonic foraminiferal $\delta^{13}C$ supports the salinity and temperature changes indicated by the $\delta^{18}O$ and suggests they were driven by a switch between proximal and distal sources. Coincident with the $\delta^{18}O$ shift, the $\delta^{13}C_{G.\ bulloides}$ began a 2 kyr depletion of 0.8‰ from 21 ka to 19 ka (Figure 6a). If regional $\delta^{13}C$ distributions were even somewhat similar to modern (Figure 1c), to sustain this change by upwelling or mixing with deeper waters would require whole-scale replacement by waters from deeper than 1000 m (Figure 1c) as well as a change in location, dynamics, and extent of upwelling from that which is found in the area today [*Zeldis et al.*, 2004]. Primary productivity removes the lighter isotopes of carbon, enriching $\delta^{13}C$ in the remaining DIC pool available to shallow subsurface foraminifera, so a drastic reduction in productivity could augment the signal, but there is no evidence for a significant change in productivity in the Bay of Plenty [*Samson et al.*, 2005; *Wright et al.*, 1995]. Across the New Zealand region, the $\delta^{13}C$ fractionation due to temperature effects on air-sea exchange is not significant today (Figure 1c) and was unlikely to be a significant factor in the deglacial record. The increased stratification we see in the Bay of Plenty water column conflicts with the possible interpretation that this signal was the result of mixing from greater depths. More likely, there was an increasing input of STMW, which is sourced through the equatorial Pacific [*Bostock et al.*, 2010].

The area north of New Zealand is a region where multiple sources for the shallow interior waters have been implicated [*Bostock et al.*, 2013]. This makes it likely that the $\delta^{13}C$ drop, beginning at 20.1 ka, resulted from a rapid increase in respired CO_2 isotopic signal caused by a change in source. We suggest the Southern Ocean proximal source, which dominated the Bay of Plenty during the glaciation by leaking in through the Tasman Sea and/or via enhanced subsurface flow and eddies around East Cape, swapped rapidly with the

early onset of Southern Hemisphere warming to contain more distal, laterally advected, subtropical components from the equatorial Pacific via the Coral Sea (Figure 8). A marked increase in Southern Ocean upwelling (Figure 7e) caused by the strengthening and southward shift of the Southern Hemisphere westerlies [*Anderson et al.*, 2009; *Toggweiler*, 1999; *Toggweiler et al.*, 2006] has been suggested to have enhanced the transfer of highly depleted preformed $\delta^{13}C$, sourced from the deep water, that was then advected north via AAIW and SAMW [*Ninnemann and Charles*, 1997; *Spero and Lea*, 2002]. Shortly after the $\delta^{13}C$ depletions seen in surface ocean waters in this study, atmospheric $\delta^{13}C$ depletion indicated this stored carbon was vented into the atmosphere [*Schmitt et al.*, 2012] (Figure 7e). We assert the shift in source waters in our study area was driven in part by these fundamental changes in Southern Ocean formation dynamics. The slow but variable $\delta^{18}O_{SW}$ and $\delta^{13}C$ enrichment toward Holocene suggests the delivery from the low latitudes persisted, with waters becoming fresher and or warmer through the deglaciation, possibly with an increasing proportion of more proximal Southern Ocean waters that were also warmer and saltier reentering the region throughout the deglaciation (Figure 6a).

The *G. inflata* stable isotopic records of deeper subsurface (upper mode) waters in the Bay of Plenty differ markedly from those of *G. bulloides*. The onset of the deglacial $\delta^{18}O_{G.\ inflata}$ depletion was coincident with the sea level increase [*Peltier and Fairbanks*, 2006] suggesting that global ice volume was the principle driver of this change. The thermocline stratification changed dramatically across this transition with a single shift to a shallower mixed layer coincident with the onset of the deglaciation (Figure 4b). These deeper $\delta^{13}C$ values were very steady with a minor depletion of less than 0.3‰ which is equivalent to the whole ocean change in $\delta^{13}C$. A small isotopic minimum at 14 ka was coincident with the global minimum $\delta^{13}C$ event described by *Spero and Lea* [2002], suggesting there was little to no change in the deep subsurface water mass sources between the LGM and the Holocene. The steadiness of this record contrasts markedly to the *G. bulloides* $\delta^{13}C$ depletion 3 kyr earlier (Figure 5), which we interpret as a shift in water mass source at the thermocline in the Bay of Plenty. The persistent enrichment in deeper layers indicates that a steady high-latitude end-member influenced the deeper subtropical subsurface water column in the New Zealand region throughout the deglaciation but the depth at which it was present appears to have shoaled along with the onset of the deglaciation.

4.2. Regional Near-Surface Circulation Changes

Our planktonic foraminiferal isotopic reconstructions suggest that during the LGM, surface and shallow interior waters in the Southwest Pacific Ocean north of New Zealand both had a different vertical structure. Additionally, the laterally advected water supplying the subsurface in the subtropics was sourced from different locations than during the Holocene. We can place the Bay of Plenty results in regional context by comparing our newly generated records with previously published high-resolution records from the area, MD97-2121, Hawke Bay [*Carter et al.*, 2008; *Marr et al.*, 2013], and MD97-2120, south Chatham Rise [*Pahnke and Zahn*, 2005] (Figure 1). Today, the position of the STF is bathymetrically fixed on the Chatham Rise [*Heath*, 1981; *Shaw and Vennell*, 2001]. Thus, Hawke Bay core MD97-2121 is bathed by the same subtropical water masses as the Bay of Plenty, whereas core MD97-2120, on the western end of the south Chatham Rise, has more polar influences with SAW present at the surface. SAMW is believed to form during winter deep mixing of surface waters on the Campbell Plateau [e.g., *Rintoul and Bullister*, 1999] and this water forms a dynamic continuum with SAW at the surface on the south Chatham Rise and with waters that ventilate the thermocline as SAMW around the North Island (Figure 1b). Reconstructions indicate that the STF remained in the same position during the LGM [*Sikes et al.*, 2002]; so the shallow thermocline dwelling foraminifera *G. bulloides* at the south Chatham Rise site can be assumed to have resided in SAW during the LGM. The signal they record can be employed as representative of local SAMW such as that formed on the Campbell Plateau [*Neil et al.*, 2004].

During the LGM, *G. bulloides* carbon isotope values on the South Chatham Rise in core MD97-2120 were relatively enriched compared to Holocene (Figure 7c) [*Charles et al.*, 2010] indicating that ventilation and proximal sourcing of SAMW in the LGM were intensified relative to today. In the Bay of Plenty and Hawke Bay, $\delta^{13}C$ values of *G. inflata* [*Carter et al.*, 2008] suggest the translation of the signal observed at the south Chatham Rise surface (as recorded by *G. bulloides* [*Charles et al.*, 2010]) to the subsurface in both Hawke Bay and the Bay of Plenty (Figures 7b and 8). Additionally, in the Bay of Plenty and Hawke Bay, the similarity in value of $\delta^{13}C_{G.\ bulloides}$ to each other and the south Chatham Rise suggests that both locations saw

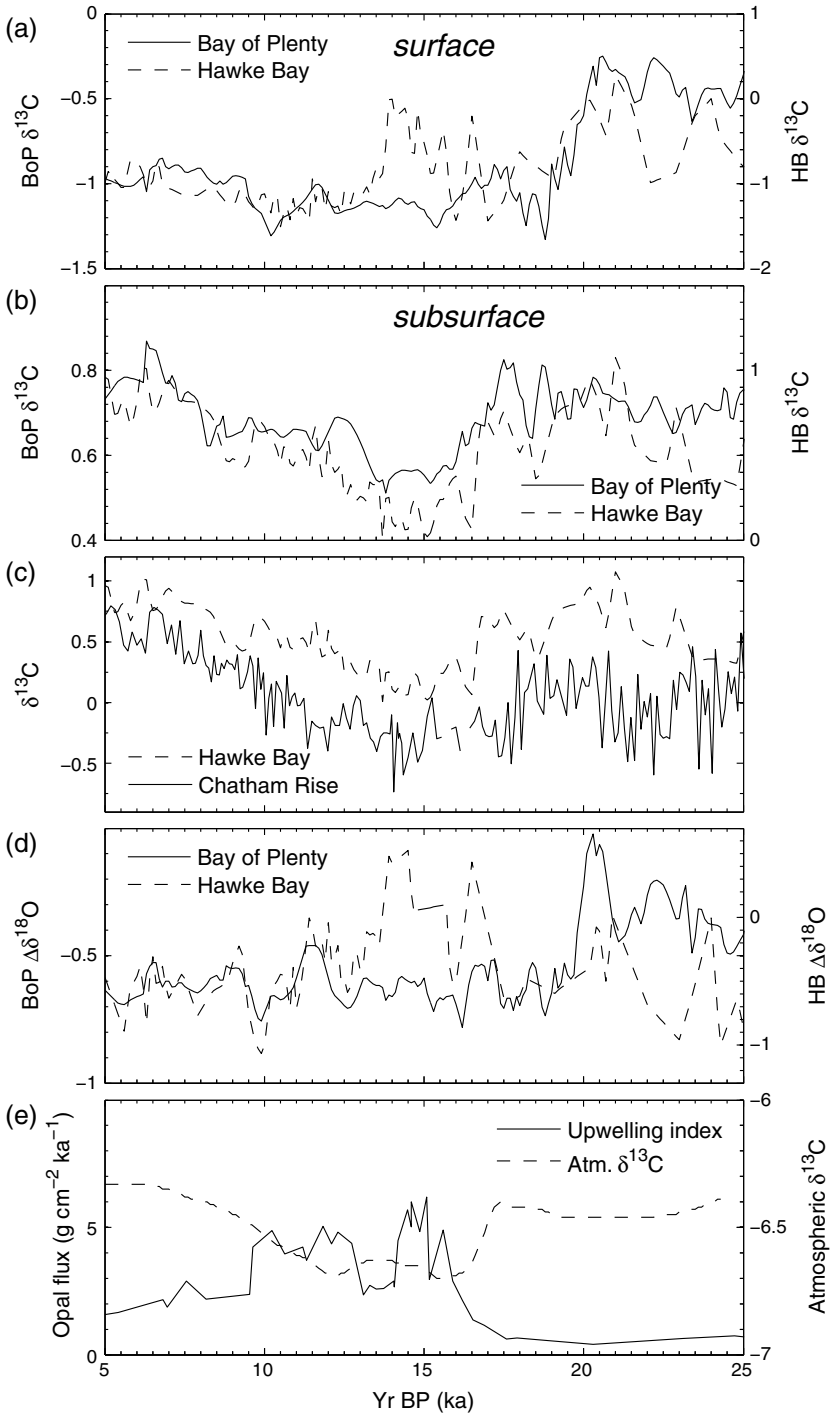

Figure 7. Compilation figure of New Zealand region and atmospheric isotopes and Southern Ocean upwelling across the deglaciation. (a) Bay of Plenty surface $\delta^{13}C_{G.\ bulloides}$ (solid; this study) and Hawke Bay surface $\delta^{13}C_{G.\ bulloides}$ (dashed) [*Carter et al.*, 2008]. (b) Bay of Plenty subsurface $\delta^{13}C_{G.\ inflata}$ (solid; this study), Hawke Bay subsurface $\delta^{13}C_{G.\ inflata}$ (dashed) [*Carter et al.*, 2008] and Chatham Rise $\delta^{13}C_{G.\ bulloides}$ (dotted). (c) Hawke Bay subsurface $\delta^{13}C_{G.\ inflata}$ (dashed) [*Carter et al.*, 2008] and Chatham Rise $\delta^{13}C_{G.\ bulloides}$ (dotted). (d) $\Delta\delta^{18}O$ as a thermocline depth indicator, Bay of Plenty (solid) and Hawke Bay (dashed). (e) Opal fluxes (solid), a proxy for Southern Ocean upwelling, from sediment core TN057-13-4PC (53°S, 5.1°E) [*Anderson et al.*, 2009], and atmospheric $\delta^{13}C$ (dashed) [*Schmitt et al.*, 2012]. In Figure 7c, note the similarity between the surface signals in subantarctic waters from south of the STF and subsurface water in Hawke Bay, suggesting a similar provenance. Surface waters in the Bay of Plenty show the same trends as Hawke Bay but to a lesser extent (note the different scales in Figures 7a and 7b). The Bay of Plenty thermocline shoaled early in the deglaciation while in Hawke Bay, the thermocline shoaled briefly at the start of the deglaciation then remained variable until the ACR. This suggests SAMW shoaled to the east of the North Island providing a possible conduit of proximal Southern Ocean sourced to the Bay of Plenty through the deglaciation.

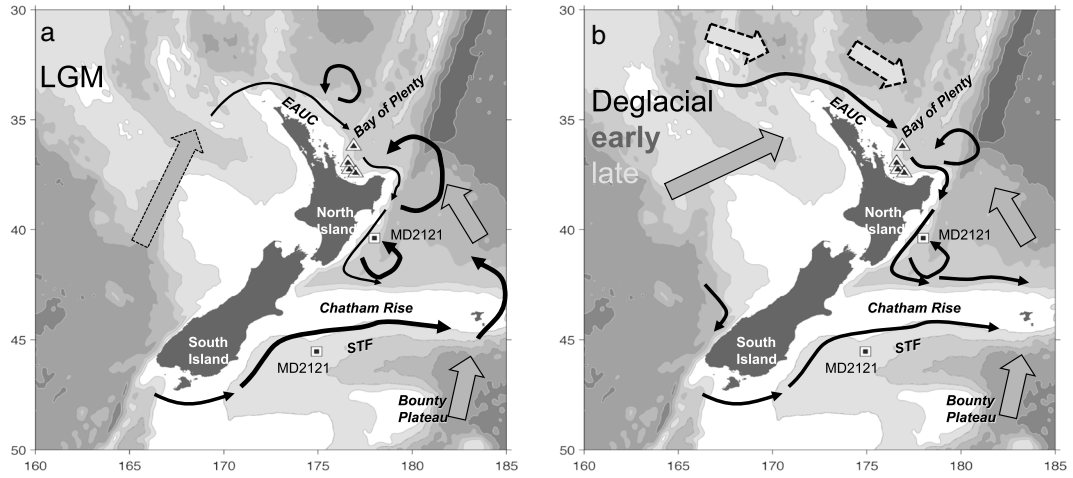

Figure 8. Schematic maps of the suggested changes in shallow circulation for (a) Last Glacial Maximum and (b) deglaciation. Surface circulation represented by black arrows and subsurface by grey. In Figure 8b, the early deglaciation is represented in dark grey arrows and later deglaciation in light grey. During the LGM, subantarctic waters were a component of surface waters in the Bay of Plenty delivered by subsurface flow from the Chatham Rise and also likely, the Tasman Sea. After the onset of deglaciation, the Bay of Plenty became increasingly influenced by distally sourced Subtropical Mode Water (STMW) delivered by flow from the west as an extension of the EAC when transport likely increased after reinvigoration of the EAC in the early deglaciation [*Sikes et al.*, 2009] that coalesces into the EAUC from the Tasman drift. Hawke Bay remained strongly influenced by SAMW until the ACR with transport from the south Chatham Rise. The deglacial increase in more tropically sourced water flowing through the Bay of Plenty resulted in a deglacial battle for competing influence of SAMW and STMW at Hawke Bay.

strengthened SAW influence in their surface waters, suggesting that waters seen at Hawke Bay [*Carter et al.*, 2008] extended their influence into the Bay of Plenty in both the mixed layer and shallow subsurface at the LGM (Figures 7b and 7c). Unlike today, water at these locations appears to have come from a proximal, high-latitude source delivered from south of the Chatham Rise, as suggested in previous studies [*Carter et al.*, 2008; *Marr et al.*, 2013]. These would have advected along a more direct path north from the STF through Hawke Bay to the Bay of Plenty, carrying with it a proximal Southern Ocean signature [*Carter et al.*, 2008], or through the Tasman Sea along the lines of modern AAIW [*Bostock et al.*, 2013] and SAMW [*Sokolov and Rintoul*, 2000], but also at shallower depths (Figure 8). This was likely due to invigorated mixing and transport dynamics such as on the Chatham Rise and Campbell Plateau to the south and are likely related to northward migration and intensification of the SAF under stronger winds and the intensification of paleocirculation around the flanks of the Campbell Plateau [*Neil et al.*, 2004]. Thus, well north of the STF, thermocline if not surface waters were influenced by SAW [*Marr et al.*, 2013] as shallow-lying SAMW [*Carter et al.*, 2002, 2008]. This has been previously suggested for Hawke Bay, but this work provides the first evidence for these influences as far north as the Bay of Plenty.

The thermocline proxy can assist in placing the source water changes in the context of transport. We calculated thermocline depth for the Hawke Bay from previously published regional *G. bulloides* and *G. inflata* $\delta^{18}O$ for comparison to the Bay of Plenty (Figure 6b). In the glacial Bay of Plenty, the thermocline was deeper than modern, while enriched $\delta^{13}C$ and $\delta^{18}O_{SW}$ values suggest this thicker mixed layer contained a greater component of proximally sourced, fresher SAMW, which is in agreement with interpretations of reduced stratification based on trace metal distributions [*Marr et al.*, 2013]. Unlike the Bay of Plenty, more negative $\Delta\delta^{18}O$ values in Hawke Bay during the early LGM indicate that the thermocline was shallow although variable, supporting interpretations from the trace metal distributions in Hawke Bay *G. bulloides* suggest reduced nutrient stratification [*Marr et al.*, 2013]. Prior to 20 ka, this was followed by a rapid but short-lived thickening of the thermocline to levels comparable to the Bay of Plenty (Figure 7d). Southern Hemisphere trade winds are suggested to have been shifted north at this time [*Russell et al.*, 2006; *Toggweiler*, 1999; *Toggweiler et al.*, 2006] likely enhancing mixing in the Bay of Plenty that only comparably influenced waters to the east of the North Island just before the transition. With southern-sourced waters present at shallower depths near Hawke Bay, a shoaled thermocline there may have allowed transport of these waters northward to become a

more integral component of the surface water mass in the Bay of Plenty. Similar dynamics in the Tasman Sea may have enhanced delivery through that route (Figure 8).

Deglacial changes in the mixed layer and the shallowest subsurface around New Zealand began early around 20–19 ka, leading Antarctic warming by ~3 ka [*Monnin et al.*, 2001]. At that time, Hawke Bay $\delta^{13}C_{G.\ bulloides}$ became depleted as in the Bay of Plenty, suggesting a shift to distally sourced subtropical waters in the shallowest layers, although this was short-lived. Simultaneously, the Hawke Bay $\Delta\delta^{18}O$ suggests the thermocline levels shoaled comparable to the Bay of Plenty (Figures 7a and 7d). Over the next ~3 kyr, a steady but low-magnitude shoaling of the thermocline in both locations persisted through the deglacial onset (Figures 6b and 7d).

Following the early deglacial changes in the mixed layer to shallowest interior waters, the deeper, subthermocline waters exhibited delayed changes at the onset of deglaciation (~17.5 ka). The less dramatic $\delta^{13}C$ depletion in the *G. inflata* record lagged the shifts in $\delta^{13}C_{G.\ bulloides}$ in both the Bay of Plenty and Hawke Bay by more than 2 kyr (Figure 5). Significantly, the shifts in the deeper foraminiferal species at both subtropical locations coincided with the more steady *G. bulloides* $\delta^{13}C$ depletion at the Chatham Rise (Figures 7b and 7c). A persistently thick thermocline existed in the Bay of Plenty only until the deglacial onset. However, Hawke Bay had a predominantly thick and fluctuating thermocline depth until the ACR. Thus, in both subtropical locations, the deglacial onset was marked by a shallow thermocline, accompanied by a shift in the deeper, subthermocline waters to a more distal source. Invigoration of the EAC early in the deglaciation [*Bostock et al.*, 2004; *Sikes et al.*, 2009] and a southward shift of the southern westerlies [*Anderson et al.*, 2009] would have strengthened subtropical inflow into the EAUC and fostered delivery of low-latitude waters to the Bay of Plenty, with extension into Hawke Bay (Figure 8). The appearance of the more tropical planktonic foraminifera *G. ruber* at around 17 ka in the deglaciation [*Carter et al.*, 2008] supports the notion that lateral transport of subtropical surface waters, possibly at a lower volume than during the Holocene, was associated with these changes.

Unlike the Bay of Plenty, which had a fairly steady thermocline depth and $\delta^{13}C$ signal through the early deglaciation (17.5 to 14.5 ka), Hawke Bay appears to have been a battleground between competing proximal subantarctic and distal subtropical influences as evidenced by the large swings in thermocline depth recorded by $\Delta\delta^{18}O$ and $\delta^{13}C$ (Figures 7a and 7b). Thus, more proximal water sources coincided with a deeper thermocline, while the shifts to distal sources coincided with shoaled thermocline depth. Similar swings are evident in the Bay of Plenty salinity reconstruction from $\delta^{18}O_{SW}$, which also imply variable input of high- to low-latitude (or fresh-salty) source shifts (Figure 6a). At Hawke Bay, a salinity reconstruction is not available but if the Bay of Plenty pattern held true for Hawke Bay, our proxies suggest there was a tradeoff between equatorial Pacific and Southern Ocean sources that played out for the duration of the early deglacial interval, recorded more clearly there than in the Bay of Plenty. This may have been associated with weak or intermittent EAUC flow after its initiation early in the deglaciation and prior to its strengthening after the ACR [*Sikes et al.*, 2009]. This midlatitude area appears to have been a sensitive area for the tracing the influence of high- versus low-latitude Southern Hemisphere forcing.

The Antarctic Cold Reversal (14.5–12.1 ka) appears to have brought a fundamental change in conditions after which the shallow waters of the Bay of Plenty and Hawke Bay attained and maintained similar isotopic signals. At Hawke Bay, the shallow surface waters shifted to distal sources and increased low-latitude influence after the ACR [*Marr et al.*, 2013] and the thermocline shoaled with deeper mixing [*Carter et al.*, 2008]. Similar influences are seen in the Bay of Plenty (Figure 8). At the same time, Hawke Bay $\delta^{13}C_{G.\ bulloides}$ became similar to the Bay of Plenty $\delta^{13}C_{G.\ bulloides}$, indicating that the shallow interior water masses shifted to modern values, interpreted as STMW taking over to continuously influence the site [*Marr et al.*, 2013]. The end of the ACR marked the invigoration of the EAC to volumes similar to modern [*Sikes et al.*, 2009]. Similarly, the EAUC increasing to modern strength, with strengthening tropical/subtropical influence, would have provided continuous delivery of low-latitude waters to Hawke Bay. Likewise, modeling studies indicate that equatorial Pacific trade winds strengthened and shifted toward a more modern position [*Bush and Philander*, 1999] at that time. The ACR appears to have been a tipping point in the subtropical Pacific, after which surface circulation and water column structure coalesced to modern patterns.

5. Conclusions

Our new multicore study of Bay of Plenty $\delta^{13}C$ and $\delta^{18}O$ records, from two planktonic foraminiferal species, *G. bulloides* and *G. inflata*, growing at different depths, provides evidence for changes in thermocline depth and source location of mixed layer and shallow subsurface waters since the LGM. During the LGM, the shallow subsurface water masses had a much greater component of regionally sourced Southern Ocean-derived (high-latitude) water. A step change occurred in the early deglaciation which resulted in shallow subsurface waters being sourced from more distant, lower latitudes, attended by a gradual shoaling of the thermocline. Nearby, in Hawke Bay, the early deglaciation played out as a battle for dominance between proximal Southern Ocean source water and distal subtropical sources with rapid and variable changes in thermocline depth and sources. The ACR appears to have been a tipping point in the transition from LGM to Holocene. After the ACR, and into the early Holocene, water column structure in the New Zealand sector of the southwest Pacific Ocean resembled modern. The firm dominance of STMW in thermocline waters across the region north of the STF is documented in the isotopic signals of the planktonic foraminifera in these sites north and east of the North Island of New Zealand. Our results identify the midlatitudes, such as the area offshore of the North Island, as a key region to decipher high- versus low-latitude influences in Southern Hemisphere shallow water masses.

Acknowledgments

We thank Susan Trimarchi and Jordan Lander for laboratory assistance, Phil Shane for assistance with tephra identification, and the University of Oregon core repository for sample collection support. We thank Jim Wright for guidance with isotopic analyses and bioturbation analysis, Richard Mortlock for guiding aspects of the sea level detrending of the $\delta^{18}O$ data, and Katharina Pahnke for providing the MD97-2120 $\delta^{13}C$ planktonic data. Our heartfelt thanks go to both Tom Guilderson for his assistance in obtaining these cores and the funding to support this work and John Wilkin for herculean efforts with figure plotting. Will Howard and Helen Bostock provided reviews. Funding for this project came from NSF OCE-0823487 and 0823549-03. Data are archived with NOAA NCDC at http://www.ncdc.noaa.gov/data-access/paleoclimatology-data.

References

Anderson, R. F., S. Ali, L. I. Bradtmiller, S. H. H. Nielson, M. Q. Fleisher, B. E. Anderson, and L. H. Burckle (2009), Wind-driven upwelling in the Southern Ocean and the deglacial rise in atmospheric CO_2, *Science*, *323*, 1441–1448.

Bé, A. W. H. (1977), An ecological, zoogeographic, and taxonomic review of Recent planktonic foraminifera, in *Oceanic Micropaleontology*, edited by A. T. S. Ramsay, pp. 1–100, Academic Press, San Diego, Calif.

Bé, A. W. H., and R. W. Gilmer (1977), A zoogeographic and taxonomic review of Euthecosomatous Pteropoda, in *Oceanic Micropaleontology*, edited by A. T. S. Ramsay, pp. 733–808, Academic, San Diego, Calif.

Bé, A. W. H., and D. S. Tolderlund (1971), Distribution and ecology of living planktonic foraminifera in surface waters of the Atlantic and Indian Oceans, in *Micropaleontology of Oceans*, edited by B. M. Funnell and W. R. Riedel, pp. 105–149, Cambridge Univ. Press, London, U. K.

Belkin, I. M., and A. L. Gordon (1996), Southern Ocean fronts from the Greenwich meridian to Tasmania, *J. Geophys. Res.*, *101*, 3675–3696, doi:10.1029/95JC02750.

Blunier, T., et al. (1998), Asynchrony of Antarctic and Greenland climate change during the last glacial period, *Nature*, *394*, 739–743.

Bostock, H. C., B. N. Opdyke, M. K. Gagan, and L. K. Fifield (2004), Carbon isotope evidence for changes in Antarctic Intermediate Water circulation and ocean ventilation in the southwest Pacific during the last deglaciation, *Paleoceanography*, *19*, PA4013, doi:10.1029/2004PA001047.

Bostock, H. C., B. N. Opdyke, and M. J. M. Williams (2010), Characterizing the intermediate depth waters of the Pacific Ocean using $\delta^{13}C$ and other geochemical tracers, *Deep Sea Res., Part I*, *57*, 847–859.

Bostock, H. C., P. J. Sutton, M. J. M. Williams, and B. N. Opdyke (2013), Reviewing the circulation and mixing of Antarctic Intermediate Water in the South Pacific using evidence from geochemical tracers and Argo float trajectories, *Deep Sea Res., Part I*, *73*, 84–98.

Bush, A. B. G., and S. G. H. Philander (1999), The climate of the Last Glacial Maximum: Results from a coupled atmosphere-ocean general circulation model, *J. Geophys. Res.*, *104*, 24,509–24,525, doi:10.1029/1999JD900447.

Carter, L., H. L. Neil, and L. Northcote (2002), Late Quaternary ice-rafting events in the SW Pacific Ocean, off eastern New Zealand, *Mar. Geol.*, *191*, 19–35.

Carter, L., B. Manighetti, G. Ganssen, and L. Northcote (2008), Southwest Pacific modulation of abrupt climate change during the Antarctic Cold Reversal-Younger Dryas, *Palaeogeogr. Palaeoclimatol. Palaeoecol.*, *260*, 284–298.

Charles, C. D., K. Pahnke, R. Zahn, P. G. Mortyn, U. Ninnemann, and D. A. Hodell (2010), Millennial scale evolution of the Southern Ocean chemical divide, *Quat. Sci. Rev.*, *29*, 399–409.

Chiswell, S. M. (1994), Variability in sea surface temperature around New Zealand from AVHRR images, *N. Z. J. Mar. Freshwater Res.*, *28*, 179–192.

Chiswell, S. M. (2003), Circulation within the Wairarapa Eddy, New Zealand, *N. Z. J. Mar. Freshwater Res.*, *37*, 691–704.

Chiswell, S. M. (2005), Mean and variability in the Wairarapa and Hikurangi Eddies, New Zealand, *N. Z. J. Mar. Freshwater Res.*, *39*(1), 121–134.

Cléroux, C., E. Cortijo, J. C. Duplessy, and R. Zahn (2007), Deep-dwelling foraminifera as thermocline temperature recorders, *Geochem. Geophys. Geosyst.*, *8*, Q04N11, doi:10.1029/2006GC001474.

Curry, W. B., and T. J. Crowley (1987), The δC of equatorial Atlantic surface waters: Implications for Ice Age pCO levels, *Paleoceanography*, *2*, 489–517, doi:10.1029/PA002i005p00489.

Curry, W. B., and D. Oppo (2005), Glacial water mass geometry and the distribution of $\delta^{13}C$ of SCO_2 in the Western Atlantic Ocean, *Paleoceanography*, *20*, PA1017, doi:10.1029/2004PA001021.

Curry, W. B., J.-C. Duplessy, L. D. Labeyrie, and N. J. Shackleton (1988), Changes in the distribution of $\delta^{13}C$ of deep water SCO_2 between the last glaciation and the Holocene, *Paleoceanography*, *3*, 317–341, doi:10.1029/PA003i003p00317.

Darling, K. F., M. Kucera, D. Kroon, and C. M. Wade (2006), A resolution for the coiling direction paradox in *Neogloboquadrina pachyderma*, *Paleoceanography*, *21*, PA2011, doi:10.1029/2005PA001189.

Field, D. B. (2004), Variability in vertical distributions of planktonic foraminifera in the California Current: Relationships to vertical ocean structure, *Paleoceanography*, *19*, PA2014, doi:10.1029/2003PA000970.

Guinasso, N. L. J., and D. R. Shink (1975), Quantitative estimates of biological mixing rates in abyssal sediments, *J. Geophys. Res.*, *80*, 3032–3043, doi:10.1029/JC080i021p03032.

Hamilton, L. (2006), Structure of the subtropical front in the Tasman, *Deep Sea Res., Part I*, *53*, 1989–2009.

Heath, R. A. (1981), The oceanic fronts around southern New Zealand, *Deep Sea Res.*, *28A*, 547–560.

Heath, R. A. (1985), A review of the physical oceanography of the seas around New Zealand, 1982, *N. Z. J. Mar. Freshwater Res.*, *19*, 79–124.
Hemleben, C., M. Spindler, I. Breitinger, and W. G. Deuser (1985), Field and laboratory studies on the ontogeny and ecology of some Globorotaliid species from the Sargasso Sea off Bermuda, *J. Foraminiferal Res.*, *15*(4), 254–272.
Hopkins, J., A. G. P. Shaw, and P. Challenor (2010), The Southland front, New Zealand: Variability and ENSO correlations, *Cont. Shelf Res.*, *30*, 1535–1548.
Hutson, W. H. (1980), Bioturbation of deep-sea sediments: Oxygen isotopes and stratigraphic uncertainty, *Geology*, *8*, 127–130.
Huybers, P., and G. Denton (2008), Antarctic temperature at orbital timescales controlled by local summer duration, *Nat. Geosci.*, *1*(11), 787–792.
King, A. L., and W. R. Howard (2001), Seasonality of foraminiferal flux in sediment traps at Chatham Rise, SW Pacific: Implications for paleotemperature estimates, *Deep Sea Res., Part I*, *48*(7), 1687–1708.
King, A. L., and W. R. Howard (2004), Planktonic foraminiferal records from Southern Ocean sediment traps: New estimates of the oceanic Suess effect, *Global Biogeochem. Cycles*, *18*, GB2007, doi:10.1029/2003GB002162.
King, A. L., and W. R. Howard (2005), δ^{18}O seasonality of planktonic foraminifera from Southern Ocean sediment traps: Latitudinal gradients and implications for paleoclimate reconstructions, *Mar. Micropaleontol.*, *56*, 1–24.
LaRiviere, J. P., A. C. Ravelo, A. Crimmins, P. S. Dekens, H. L. Ford, M. Lyle, and M. W. Wara (2012), Late Miocene decoupling of oceanic warmth and atmospheric carbon dioxide forcing, *Nature*, *486*, 97–100.
Lisiecki, L. E., and M. E. Raymo (2005), A Pliocene-Pleistocene stack of 57 globally distributed benthic δ^{18}O records, *Paleoceanography*, *20*, PA1003, doi:10.1029/2004PA001071.
Loubere, P., and S. Bennett (2008), Southern Ocean biogeochemical impact on the tropical ocean: Stable isotope records from the Pacific for the past 25,000 years, *Global Planet. Change*, *63*(4), 333–340.
Lowe, D. J., M. Blaauw, A. G. Hogg, and R. W. Newnham (2013), Ages of 24 widespread tephras erupted since 30,000 years ago in New Zealand, with re-evaluation of the timing and palaeoclimatic implications of the late glacial cool episode recorded at Kaipo bog, *Quat. Sci. Rev.*, *74*, 170–194.
Marr, J. P., L. Carter, H. C. Bostock, A. Bolton, and E. Smith (2013), Southwest Pacific Ocean response to a warming world: Using Mg/Ca, Zn/Ca, and Mn/Ca in foraminifera to track surface ocean water masses during the last deglaciation, *Paleoceanography*, *28*, 347–362, doi:10.1002/palo.20032.
McCartney, M. S. (1977), Subantarctic mode water, in *A Voyage of Discovery*, edited by M. V. Angel, pp. 103–119, Deep-Sea Research (suppl.), Pergammon, New York.
Monnin, E., A. Indermuhle, A. Dallenbach, J. Fluckiger, B. Stauffer, T. F. Stocker, D. Raynaud, and J.-M. Barnola (2001), Atmospheric CO_2 concentrations over the last glacial termination, *Science*, *291*, 112–114.
Mook, W. G., J. C. Bommerson, and W. H. Staverman (1974), Carbon isotope fractionation between dissolved bicarbonate and gaseous carbon dioxide, *Earth Planet. Sci. Lett.*, *22*, 169–176.
Neil, H. L., L. Carter, and M. Y. Morris (2004), Thermal isolation of Campbell Plateau, New Zealand, by the Antarctic Circumpolar Current over the past 130 kyr, *Paleoceanography*, *19*, PA4008, doi:10.1029/2003PA000975.
Ninnemannn, U., and C. D. Charles (1997), Regional differences in Quaternary subantarctic nutrient cycling: Link to intermediate and deep water ventilation, *Paleoceanography*, *12*, 560–567, doi:10.1029/97PA01032.
Orsi, A., T. Whitworth, and W. D. Nowlin (1995), On the meridional extent and fronts of the Antarctic Circumpolar Current, *Deep Sea Res.*, *42*, 641–673.
Pahnke, K., and J. P. Sachs (2006), Sea surface temperatures of southern midlatitudes 0–160 kyr B.P., *Paleoceanography*, *21*, PA2003, doi:10.1029/2005PA001191.
Pahnke, K., and R. Zahn (2005), Southern hemisphere water mass conversion linked with North Atlantic climate variability, *Science*, *307*, 1741–1746.
Pahnke, K., R. Zahn, H. Elderfield, and M. Schulz (2003), 340,000-year centennial-scale marine record of southern hemisphere climatic oscillation, *Science*, *301*(5635), 948–952.
Peltier, W. R., and R. G. Fairbanks (2006), Global glacial ice volume and Last Glacial Maximum duration from an extended Barbados sea level record, *Quat. Sci. Rev.*, *25*, 3322–3337.
Peng, T.-S., and W. S. Broecker (1984), The impacts of bioturbation on the age difference between benthic and planktonic foraminifera in deep sea sediments, *Nucl. Instrum. Methods Phys. Res., Sect. B*, *5*, 346–352.
Ridgway, K. R., and J. R. Dunn (2007), Observational evidence for a Southern Hemisphere oceanic supergyre, *Geophys. Res. Lett.*, *34*, L13612, doi:10.1029/2007GL030392.
Ridgway, K. R., and K. Hill (2009), The East Australian Current, in *A Marine Climate Change Impacts and Adaptation Report Card for Australia 2009*, edited by E. S. Poloczanska, A. J. Hobday, and A. J. Richardson, Natl. Clim. Change Adapt. Res. Fac., Cleveland, Ohio.
Rintoul, S. R., and J. L. Bullister (1999), A late winter hydrographic section from Tasmania to Antarctica, *Deep Sea Res., Part I*, *46*(8), 1417–1454.
Roemmich, D., and P. Sutton (1998), The mean and variability of ocean circulation past northern New Zealand: Determining the representatives of hydrographic climatologies, *J. Geophys. Res.*, *103*, 13,041–13,054, doi:10.1029/98JC00583.
Rose, K. R., E. L. Sikes, T. P. Guilderson, P. A. Shane, T. M. Hill, R. Zahn, and H. J. Spero (2010), Upper-ocean-to-atmosphere radiocarbon offsets imply fast deglacial carbon dioxide release, *Nature*, *466*, 1093–1097.
Russell, J. L., K. W. Dixon, A. Gnanadesikan, R. J. Stouffer, and J. R. Toggweiler (2006), Southern Ocean Westerlies in a warming world: Propping open the door to the deep ocean, *J. Clim.*, *19*, 6382–6390.
Sallée, J.-B., K. Speer, S. Rintoul, and S. Wijffels (2010), Southern Ocean thermocline ventilation, *J. Phys. Oceanogr.*, *40*(3), 509–529, doi:10.1175/2009JPO4291.1.
Samson, C. R., E. L. Sikes, and W. R. Howard (2005), Deglacial paleoceanographic history of the Bay of Plenty, New Zealand, *Paleoceanography*, *20*, PA4017, doi:10.1029/2004PA001088.
Schmitt, J., et al. (2012), Carbon isotope constraints on the deglacial CO_2 rise from ice cores, *Science*, *336*, 711–714.
Shackleton, N. J. (1974), Attainment of isotopic equilibrium between ocean water and the benthonic foraminifera genus Uvigerina: Isotopic changes in the ocean during the last glacial, in *Les méthodes quantitatives d'étude des variations du climat au cours du Pléistocene*, edited by J. Labeyrie, pp. 203–209, Gif-sur-Yvette Colloques Int. duc. N. R. S.
Shakun, J. D., P. U. Clark, F. He, S. A. Marcott, A. C. Mix, Z. Liu, B. Otto-Bliesner, A. Schmittner, and E. Bard (2012), Global warming preceded by increasing carbon dioxide concentrations during the last deglaciation, *Nature*, *484*, 49–55.
Shane, P. A., E. L. Sikes, and T. P. Guilderson (2006), Tephra beds in deep-sea cores off northern New Zealand: Implications for the history of Taupo Volcanic Zone, Mayor Island, and White Island volcanoes, *J. Volcanol. Geotherm. Res.*, *154*(4), 276–290.
Shaw, A. G. P., and R. Vennell (2001), Measurements of an oceanic front using a front-following algorithm for AVHRR SST imagery, *Remote Sens. Environ.*, *75*(1), 47–62.

Sigman, D. M., M. P. Hain, and G. H. Haug (2010), The polar ocean and glacial cycles in atmospheric CO_2 concentration, *Nature*, *466*, 47–55.
Sikes, E. L., and L. D. Keigwin (1994), Equatorial Atlantic sea surface temperatures for the last 30 kyr: A comparison of U^k_{37}, $\delta^{18}O$, and foraminiferal assemblage temperature estimates, *Paleoceanography*, *9*, 31–45, doi:10.1029/93PA02198.
Sikes, E. L., and L. D. Keigwin (1996), A reexamination of northeast Atlantic sea surface temperature and salinity over the last 16 kyr, *Paleoceanography*, *11*, 327–342, doi:10.1029/95PA03697.
Sikes, E. L., C. R. Samson, T. P. Guilderson, and W. R. Howard (2000), Old radiocarbon ages in the southwest Pacific Ocean during the last glacial period and deglaciation, *Nature*, *405*, 555–559.
Sikes, E. L., W. R. Howard, H. L. Neil, and J. K. Volkman (2002), Glacial-interglacial sea surface temperature changes across the subtropical front east of New Zealand based on alkenone unsaturation ratios and foraminiferal assemblages, *Paleoceanography*, *17*(2), 1012, doi:10.1029/2001PA000640.
Sikes, E. L., W. R. Howard, C. R. Samson, T. S. Mahan, L. G. Robertson, and J. K. Volkman (2009), Southern Ocean seasonal temperature and Subtropical Front movement on the South Tasman Rise in the Late Quaternary, *Paleoceanography*, *24*, PA2201, doi:10.1029/2008PA001659.
Sloyan, B. M., and S. R. Rintoul (2001), Circulation, renewal, and modification of Antarctic mode and intermediate water, *J. Phys. Oceanogr.*, *31*(4), 1005–1030.
Sokolov, S., and S. Rintoul (2000), Circulation and water masses of the southwest Pacific: WOCE Section P11, Papua New Guinea to Tasmania, *J. Mar. Res.*, *58*, 223–268.
Sowers, T., and M. Bender (1995), Climate records covering the last deglaciation, *Science*, *269*, 210–214.
Spero, H. J., and D. W. Lea (2002), The cause of carbon isotope minimum events on glacial terminations, *Science*, *296*, 522–525.
Spero, H. J., K. M. Mielke, E. M. Kalve, D. W. Lea, and D. K. Pak (2003), Multispecies approach to reconstructing eastern equatorial Pacific thermocline hydrography during the past 360 kyr, *Paleoceanography*, *18*(1), 1022, doi:10.1029/2002PA000814.
Stott, L., A. Timmermann, and R. Thunell (2007), Southern Hemisphere and deep-sea warming led deglacial atmospheric CO_2 rise and tropical warming, *Science*, *318*, 435–438.
Thompson, P. R., and N. J. Shackleton (1980), North Pacific palaeoceanography: Late Quaternary coiling variations of planktonic foraminifer *Neogloboquadrina pachyderma*, *Nature*, *287*, 829–833.
Thornalley, D. J. R., H. Elderfield, and N. McCave (2009), Holocene oscillations in temperatures and salinity of the surface subpolar North Atlantic, *Nature*, *457*, 711–714.
Toggweiler, J. R. (1999), Variation of atmospheric CO_2 by ventilation of the ocean's deepest water, *Paleoceanography*, *14*, 571–588, doi:10.1029/1999PA900033.
Toggweiler, J. R., J. L. Russell, and J. R. Carson (2006), Mid-latitude westerlies, atmospheric CO_2, and climate changes during the ice ages, *Paleoceanography*, *21*, PA2005, doi:10.1029/2005PA001154.
Tsuchiya, M., and L. D. Talley (1996), Water property distributions along an eastern Pacific hydrographic section at 1351 W, *J. Mar. Res.*, *54*, 541–564.
Vandergoes, M. J., et al. (2013), A revised age for the Kawakawa/Oruanui tephra, a key marker for the Last Glacial Maximum in New Zealand, *Quat. Sci. Rev.*, *74*(1-7), 195–201.
Wright, I. C., M. S. McGlone, C. S. Nelson, and B. J. Pillans (1995), An integrated latest Quaternary (stage 3 to present) paleoclimatic and paleoceanographic record from offshore northern New Zealand, *Quat. Res.*, *44*, 283–293.
Zeldis, J. R., R. A. Walters, M. J. N. Greig, and K. Image (2004), Circulation over the northeastern New Zealand continental slope, shelf, and adjacent Hauraki Gulf during spring and summer, *Cont. Shelf Res.*, *24*, 543–561.